

Solar Powered Engine Based on Unijunction Transistors

W. Abd El-Basit^{1*}, Z. I. M. Awad¹, S. A. Kamh¹ and F. A. S. Soliman²
¹(Physics Dept., Faculty of Women for Arts, Science, and Education, Ain-Shams University, Cairo, Egypt)
²(Nuclear Materials Authority, P.O.Box 530, Maadi-11728, Cairo, Egypt)

Abstract : The present paper is a trial to shed further light on one of the state - of the - art applications of solar energy; that is solar engines. In this concern, the unijunction transistors were introduced as a part of the system control, where, the solar engines have broad significant and technological advantages for distributed renewable energy applications. During this paper, a detailed experimental study of the characteristics of one of the most popular 2N4870 UJT's was investigated in normal operating conditions. Also, the electrical characteristic curves of the investigated poly-silicon solar panel were plotted at different illumination levels. The design and the implementation of the solar engine control circuit as an application were carried out. Finally, the dependence of both output voltage and motor speed of the solar engine control circuit on the illumination level were investigated.

Keywords: Unijunction transistor, emitter electrical characteristics, applications, solar panel and solar engine.

I. Introduction

Today we are moving toward the use of natural resources for the energy generation [1]. With the increasing population of the world, researchers should think about alternate sources of energy because primary sources of fuel are limited in stock (Fig. 1a). Noting that Egypt lies in the highest level of solar radiation belts (Fig. 1b). So, the scientists are looking for sustainable energy sources like sun, wind, water and tidal flow. Of them solar energy is the prime source of renewable energy as it can get easily from nature [2]. Mass production and use of electricity generated from solar energy has recently become more common, perhaps because of the environmental threats arising from the production of electricity from fossil fuels and nuclear power [3]. With recent technological advances in Renewable Energy (RE), solar energy may be gaining ground compared to fossil fuels for its environmental benefits through reduced use of fossil fuels, reducing problems associated with pollution and global warming, resulting in cleaner air and cleaner water [4]. A wide variety of technologies to convert solar radiation into useful energy in form of heat or electricity have been developed [5]. Solar cells represent the fundamental power conversion unit of a photovoltaic system. They are made from semiconductors and have much in common with other solid-state devices, such as diodes, transistors and integrated circuits. They are usually assembled into modules for practical operation [6]. Finally, in this concern, this paper presents the design, analysis, and implementation of solar engine system based on unijunction transistors.

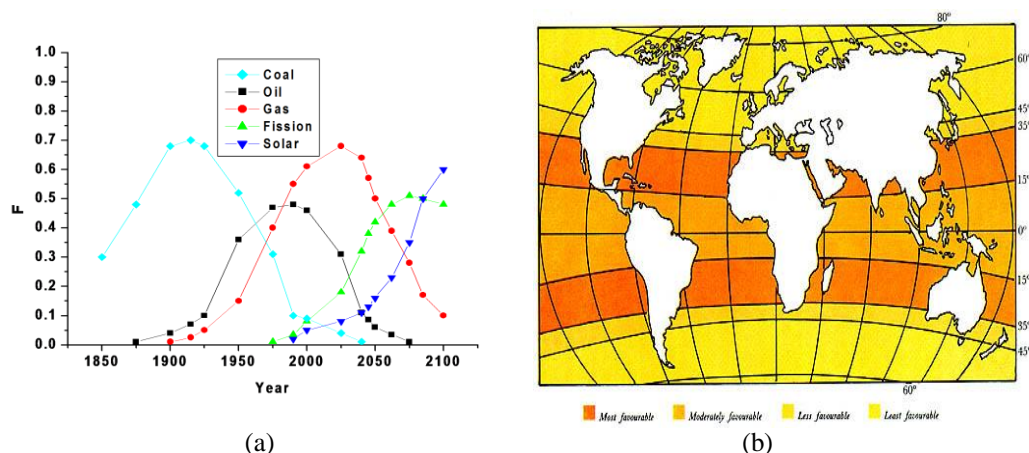


Fig. (1). (a) Energy sources for the history and projection of world and (b) world distribution of solar radiation into belts indicating feasibility of solar applications.

1.1 Over View of Unijunction Transistor

The unijunction transistor is a three terminal semiconductor device, in which a $p-n$ junction- called injector- is created (Fig. 2a). It divided the device into two base regions (B_1 , B_2). Their resistivity varies owing to carrier injection. Due to this, on the characteristics of unijunction transistor appears a domain with negative resistance, that is, under certain conditions, the voltage across the transistor can be reduced even with an increase in the output current through the load of transistor (Fig. 2b). Only the turn off transistor or opening the circuit can remove the input voltage [7]. Because of this, unijunction transistors are used in pulse generators, sawtooth generators, threshold devices, and converters. Circuits based on unijunction transistors are simpler and more reliable than those built around diode-connected and bipolar transistors [8]. It also finds applications in triggering circuits of thyristors (Silicon controlled rectifier, Triac,.... etc.) in power industry to control large AC current [9].

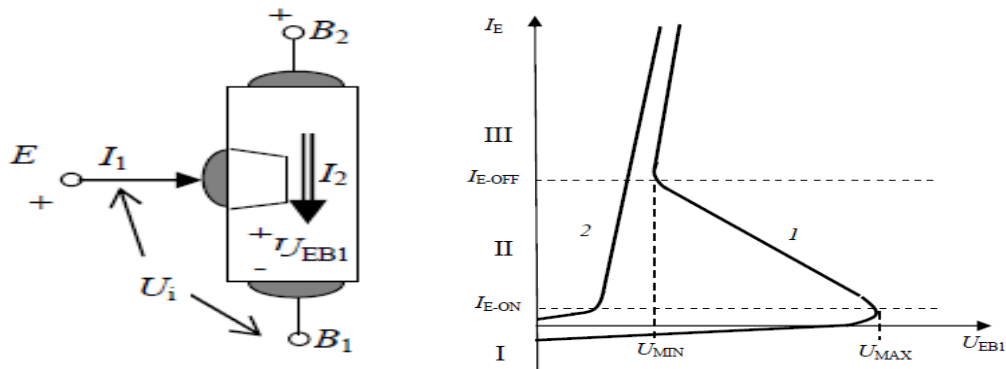


Fig. (2). Scheme of unijunction transistor (a) and its characteristic curve (b).

1.2 Solar Engine

The first solar engine was built by Tilden in late 1989 [10, 11]. Solar Engine (SE) circuit is a circuit that takes in and stores electrical energy from solar cells, and when a predetermined amount has accumulated, it switches on to drive a motor or other actuator (Fig. 3) [12-15]. SE provides usable mechanical energy when only meagre or weak levels of sunlight, or artificial room light, are present. It harvests or gathers, as it were, bunches of low grade energy until there is enough for an energy giving meal for a motor. And when the motor has expended the serving of energy, SE circuit goes back into its gathering mode. It is an ideal way to intermittently power models, toys, or other small gadgets on very low light levels.



Fig. (3). Simple solar engines.

Solar Engine circuit is in principle a control circuit that takes micro power (milliamps of current) and converts into more powerful pulses (Fig. 4). These are usually used to power motors, but can be used to power other motion-creating devices, such as, Nitinol wire.

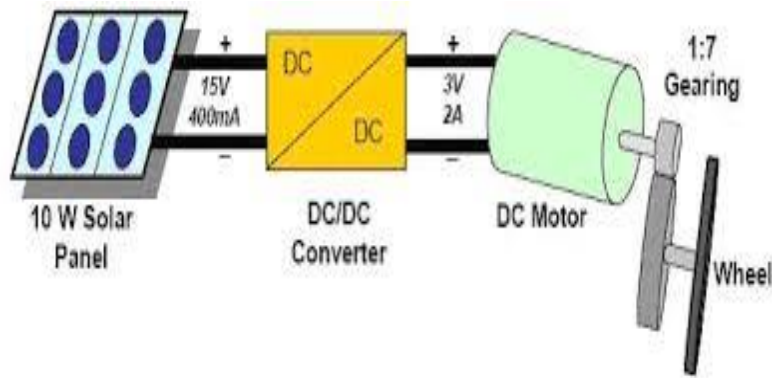


Fig. (4). Solar engine circuit as a control circuit that takes micro power and converts it into more powerful pulses.

The investigated solar engine turns on when the current going into the capacitor drops below a certain threshold. In bright light, SE will turn on at a high voltage, and in low light it will turn on at a much reduced voltage, because there isn't as much current available. The solar engine is an on board power plant for BEAM (Biology, Electronics, Aesthetics, and Mechanics) type robots (Fig. 5), sometimes called living robots [16, 17].

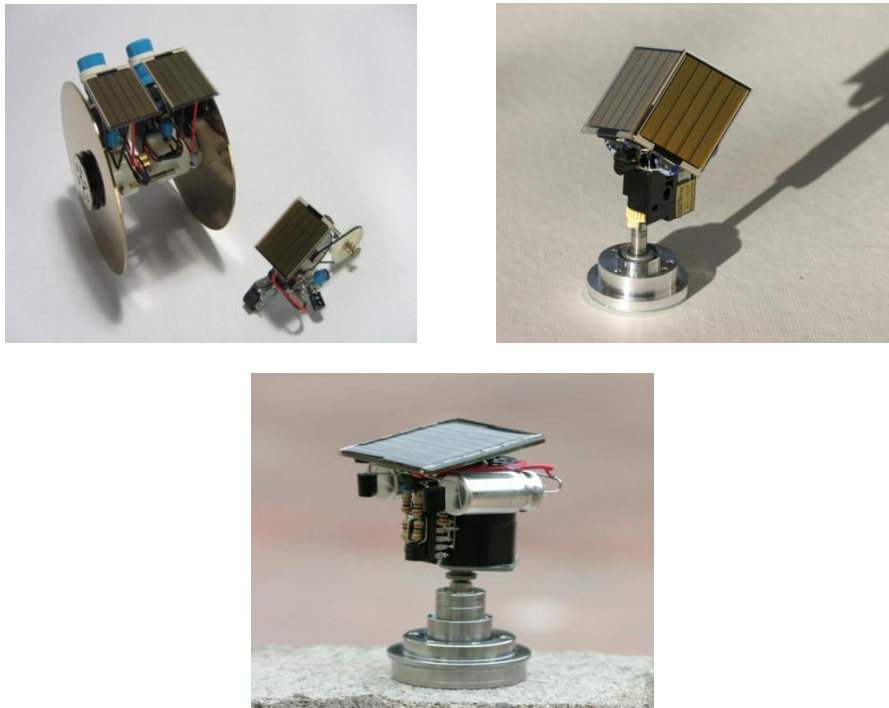


Fig. (5). BEAM type Robots.

II. Experimental Work

During the present paper detailed experimental study of the electrical characteristics of one of the most popular 2N4870 UJTs are investigated in normal operating conditions. In this concern, the static and dynamic characteristics of this device, as well as, emitter characteristics and interbase characteristics, of UJT are studied. From which, the interbase resistance of UJT is determined. The experimental set up, shown in Fig. (6) is used for studying the emitter characteristic curves of the proposed UJTs.

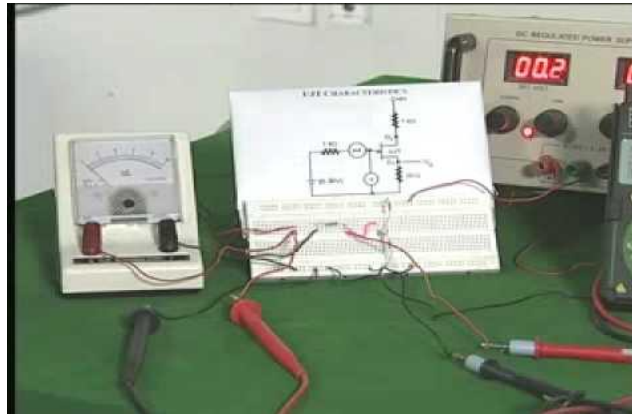


Fig. (6). Experimental set up used for the characterization of UJTs.

The current-voltage, and power-voltage characteristic curves of the investigated polycrystalline silicon solar panel, plotted at different illumination levels, as well, the illumination level dependence of solar engine control unit output voltage and motor speed, the design, and implementation of the proposed solar engine system are carried out. In this concern, Fig. (7) shows the solar engine circuits based on UJT, and UJT and SCR, also, Figs. (8 and 9) show their implementation steps of both systems. Finally, the principle operation of SE can be summarized as follows:

- The solar panel charges the main 4700 μF capacitor,
- As the capacitor charges, voltage level of the circuit increases.
- The UJT begins oscillating and sending a trigger pulse to the Q1.
- When the circuit voltage has risen to about 2.0 Volts from the main capacitor, the trigger pulse is sufficient to turn on the Q1.
- When Q1 turns on, this turns on Q2 the 2N3906 transistor through the 2.2 k Ω resistor.
- The 2N3906 keeps the 2N3904 turned on until all the store power in the main capacitor is dumped through the 2N3904 and the high efficiency (DC) motor.
- The motor spins momentarily as the capacitor discharges then stops, the cycle repeats.

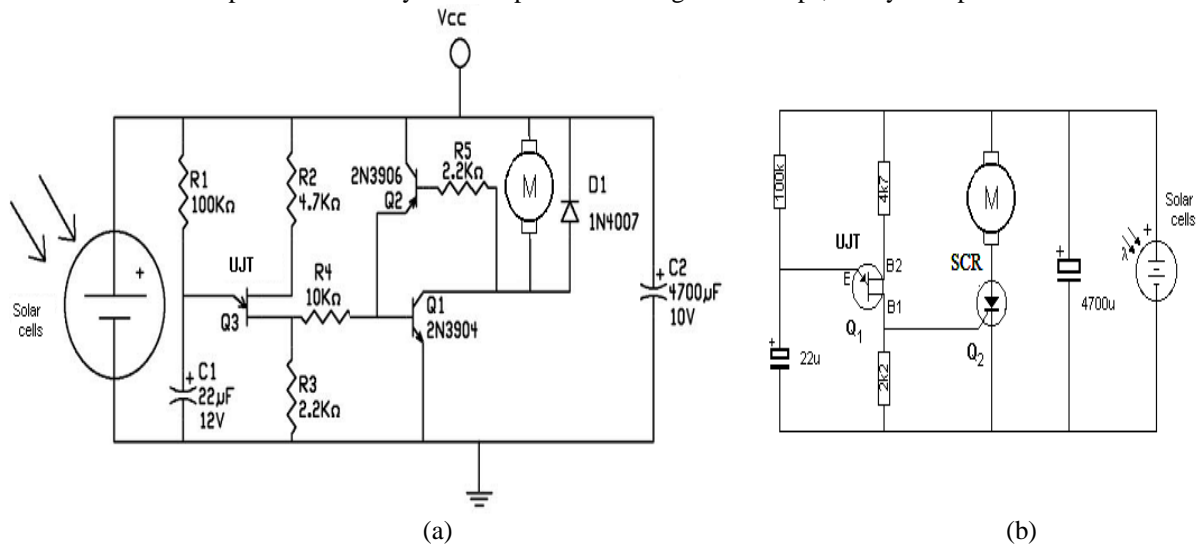


Fig. (7). Experimental solar engine circuit based on (a) UJT and (b) UJT and SCR.



Fig. (8). Prototype solar engine based on UJT.



Fig. (9). Prototype solar engine based on UJT and SCR.

III. Results and Discussions

3.1 Static Characteristics of UJTs

3.1.1 Emitter Characteristics

The static emitter characteristic curves (I_E - V_E) of UJTs are plotted at different interbase voltage (V_{B1B2}) values of 0.0, 2.0, 4.0, 6.0, 8.0, 10 and 15 Volts, respectively (Fig. 10). From which, it is clear that for applied emitter voltage V_E values smaller than the peak-point voltage, V_P , the p-n junction at the emitter is reverse-biased and only a small leakage current normally flows in the emitter, this region is called the cut off region [18, 19]. When the voltage V_E is increased, a voltage is reached where, V_E is equal to the sum of forward voltage drop across the p-n junction and the voltage across, R_{B1} . This voltage is known as the peak-point voltage, V_P , or firing-point voltage. When the applied V_E reaches the firing potential, V_P , the diode will fire and UJT will conduct from the cut off region into the negative resistance region. The emitter firing potential is given by [20]:

$$V_P = \eta V_{B1B2} + V_D \dots \dots \dots (1)$$

Where

- η : intrinsic standoff ratio of UJT, is typically within the range of 0.5 to 0.85,
- V_{B1B2} : interbase voltage,
- V_D : forward voltage drop across the diode, is typically 0.70 Volt.

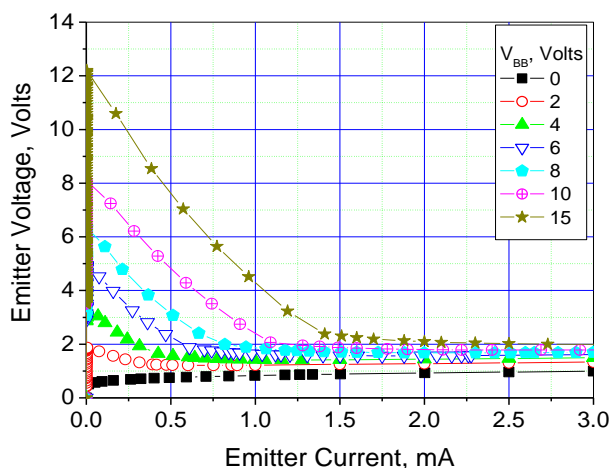


Fig. (10). Static emitter characteristic curves of 2N4870 UJTs, plotted at different interbase voltage values.

As the emitter-base1 voltage comes higher than V_P , the p-n junction is forward-biased. So, holes are injected from the emitter into the silicon bar. Since B_1 is negative with respect to the emitter, the electrical field is such that most holes move towards the B_1 terminal. An equal number of electrons are injected from B_1 to maintain electrical neutrality in the bar. The increase in current carried in the silicon bar decreases the value of R_{B1} . This causes the fraction of voltage across R_{B1} to decrease, which causes a further increase of emitter current I_E and a lower resistance for R_{B1} . The region between the peak point voltage V_P and the valley-point voltage V_V is called “negative resistance region”.

Figure (11a) shows the interbase voltage dependence of peak - and valley -voltages, it is clear that V_P is proportional to the magnitude of V_{B1B2} , where, as V_{B1B2} increases, V_V increases, following linear fit. Figure (11b) shows the interbase voltage dependence of peak - and valley -currents, considering I_P , which can be defined as the minimum emitter current required to fire UJT. I_P is found to be inversely proportional to V_{B1B2} , following 1st order exponential decay fitting. Also, I_V increases linearly with increasing interbase voltage, following a linear fit. Finally, Figs. (11c and 11d) show the interbase voltage dependence of the negative differential resistance and intrinsic standoff ratio are shown to be approximately linear ascending functions.

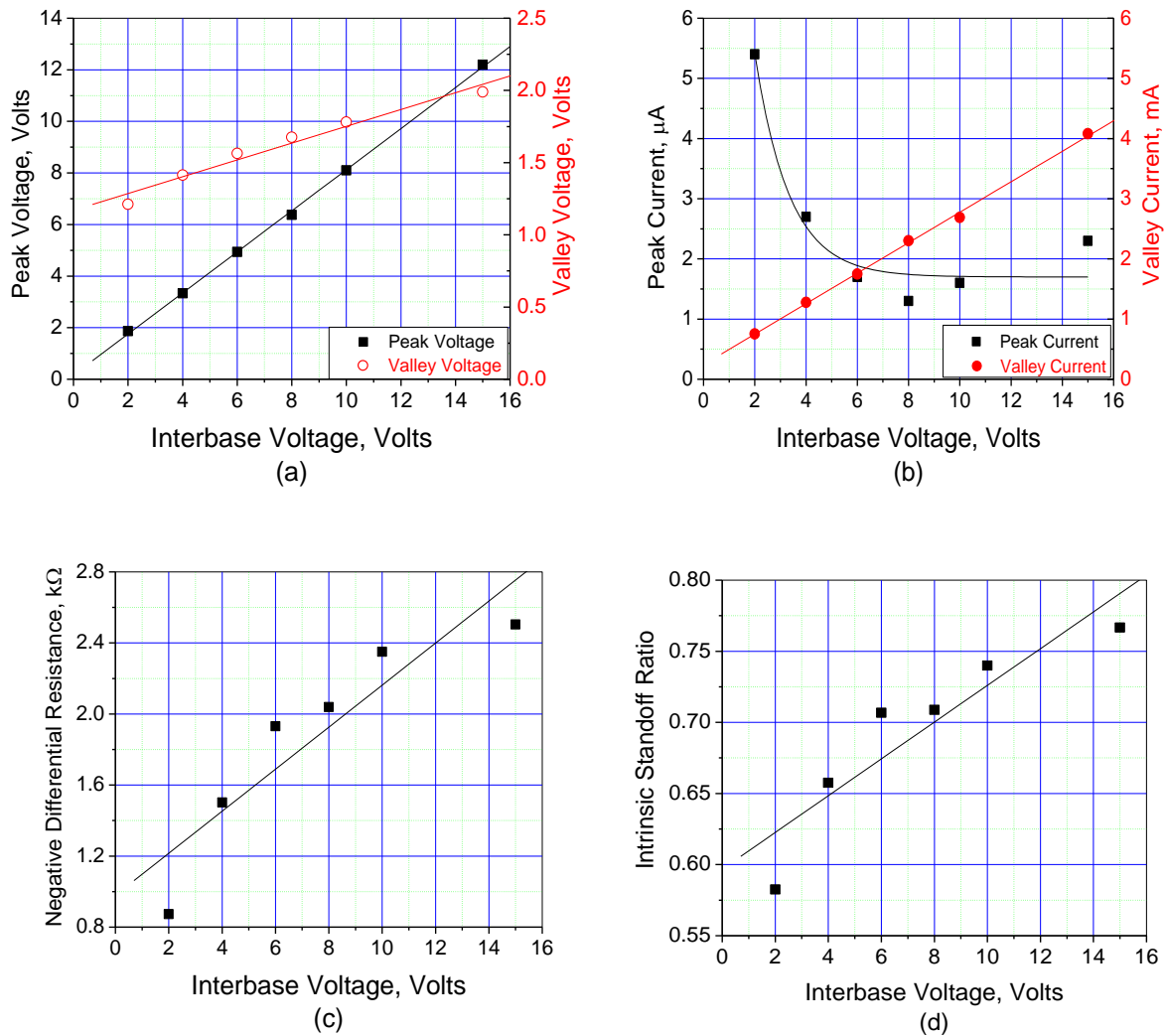


Fig. (11). (a) Interbase voltage dependence of peak - and valley -voltages, (b) peak- and valley- currents, (c) negative differential resistance and (d) intrinsic standoff ratio of 2N4870 UJTs.

3.1.2 Interbase Characteristics of UJTs

One of the very important characteristics of UJT is the interbase characteristics. In this concern, Fig. (12) shows the interbase characteristics, plotted at different emitter current I_E values of 0, 2.0, 5.0, 10, 15 and 20 mA, respectively. The given relationships are shown to be similar to the collector characteristic of a conventional transistor. From which, it is shown that base current increase with increasing interbase voltage.

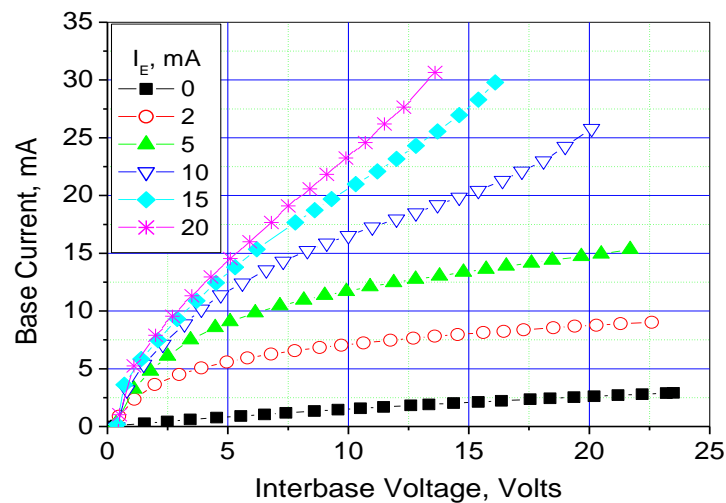


Fig. (12). Interbase voltage dependence of base current, plotted at different emitter current values.

3.1.3 Determination of the Interbase Resistance of UJT

In case of emitter open, interbase resistance (R_{BB}) of UJT can be determined. It is shown from Fig. (13) that the base current increases linearly with increasing interbase voltage, following a linear fit. From which, the interbase resistance (R_{BB}) of UJT is calculated, where its value is shown to be around 7.27 k Ω .

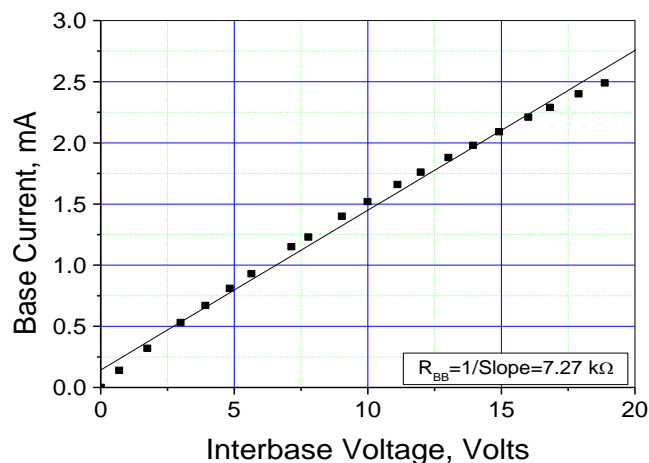


Fig. (13). Interbase voltage dependence of base current of 2N4870 UJTs.

3.2 Solar Engine

During the present part of the paper, solar engine (BEAM-type robots) based on UJT circuit and system is investigated. In this concern, and referring to Fig. (7a), the given solar engine circuit is applied, where the main components of the system are:

- solar cell/panel,
- main capacitor,
- slow oscillating or trigger circuit, and
- dc-motor.

3.2.1 Solar Panel

Figure (14) shows a polycrystalline silicon solar panel with area of 96.32 cm which is used [21-23], where its electrical characteristics are:

- Solar panel polycrystalline DIY small cell charger
- Transfer efficiency not less than 17%,

- Dimension : 112×84 mm, and
- 6.0 Volts, at 200 mA, and 1.10 Watts.



Fig. (14). Polycrystalline silicon solar panel.

The current-voltage, and power-voltage - characteristic curves of the investigated Polycrystalline silicon solar panel, plotted at different illumination levels are shown in Fig. (15). Table (1) summaries the approximated or averaged values of the main electrical parameters of the panel, obtained at illumination level of 24 klux.

Table (1). Electrical characteristics of polycrystalline silicon solar panel with area of 96.32 cm², plotted at 24 klux.

Test Sample	I _{SC} , mA	V _{OC} , V	P _{MAX} , mW
Polycrystalline Si-panel, 96.32 cm ²	200	5.39	504.25

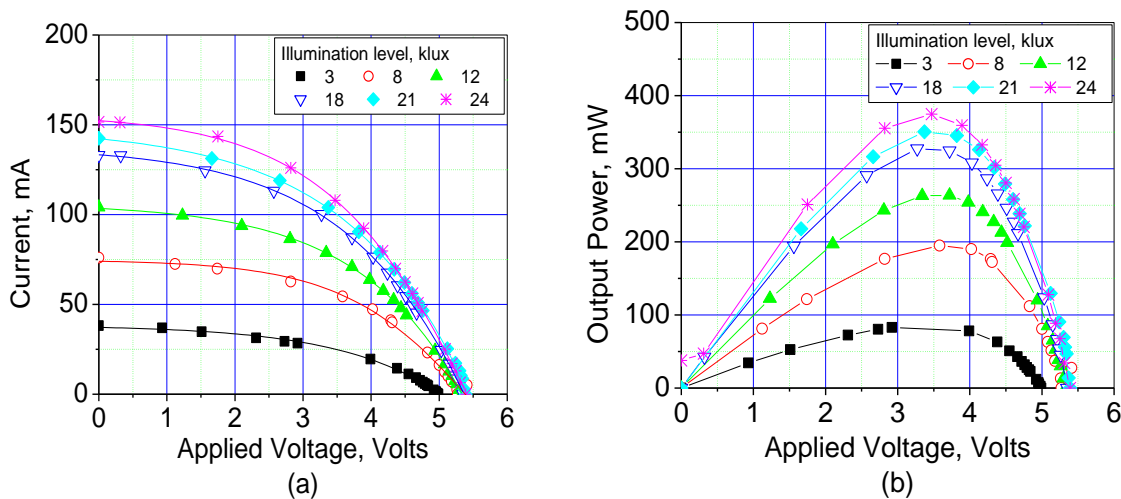


Fig. (15). (a) Output (I-V) - and (b) output (P-V) - characteristic curves of polycrystalline silicon solar panel with area of 96.32 cm², plotted at different illumination levels.

3.2.2 Output Characteristics of Solar Engine

In order to shed further light on the importance of the solar cell applications and operation of the solar engine, the following part of the paper is mainly concerned with studying the effect of solar illumination on the output of the solar engine control circuit, and its motor speed. In this concern, Fig. (16) shows the illumination level dependence of solar engine control circuit output voltage and motor speed. From which, it is clear that a linear dependence is obtained with correlation values better than 0.99 for both cases.

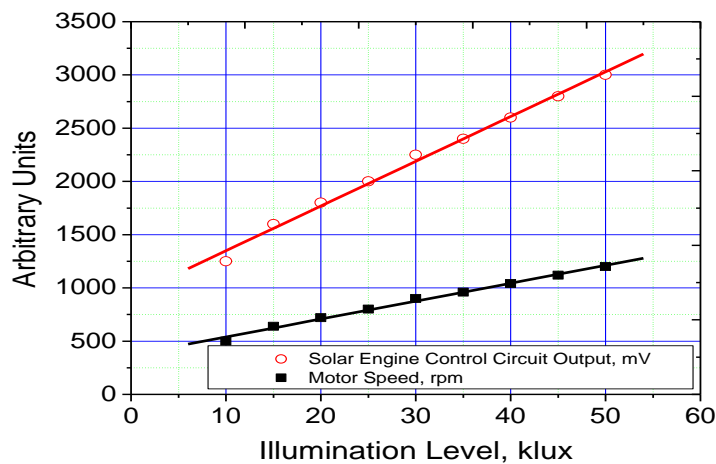


Fig. (16). Illumination level dependence of solar engine control output voltage and motor speed.

3.2.3 Solar Based Power Motors

If the solar panel is directly to a dc electrical motor, then the solar panel is sending power directly to the motor and the motor is using the electrical energy immediately. In this case the motor is "Directly Powered by Solar Energy" (Fig. 17a). On the other hand, if the solar panel is connected in a parallel circuit with a motor and a battery then the solar panel will charge the battery and the dc motor will get dc electrical energy from the battery. The energy used to power the motor came from the battery. However, the energy in the battery came from solar energy so we say that the motor is "Indirectly Powered by Solar Energy" (Fig. 17b).

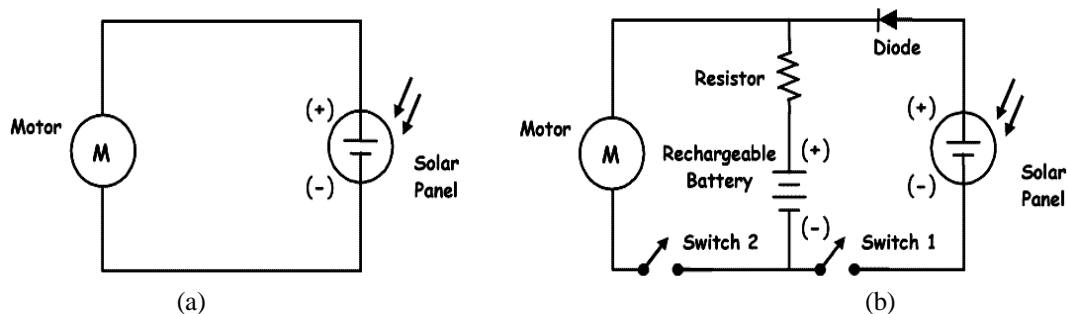


Fig. (17). Solar powered DC electrical motor: directly and indirectly powered.

IV. Conclusion

From the study, analysis, design, and implementation of a prototype solar engine system, it is proved that solar energy is of great role on such field. The matter is due to that solar is a source of infinite clean and stable energy. Especially in the countries which are characterized by the high level and consistency solar energy throughout the day and year time. Finally, the proposed system has proved successful and good sensitivity and is the nucleus of the practical applications on a large scale in all air and maritime transport areas, where large areas of solar panels could be applied, especially on outer space.

References

- [1] Sunny Tak, Ravi Prakash Sharma and Sunil Yadav, Comparison Between Solar Stirling Engine and other Solar Devices, Proc. 5th SARC-IRF International Conf., New Delhi, India, 2014, 6-8.
- [2] Khizir Mahmud, Sayidul Morsalin and Md. Imran Khan, Design and Fabrication of an Automated Solar Boat, International Journal of Advanced Science and Technology, 64, 2014, 31-42.
- [3] Dzung Nguyen and Brad Lehman, An Adaptive Solar Photovoltaic Array Using Model-Based Reconfiguration Algorithm, IEEE Transactions on Industrial Electronics, 55(7), July 2008, 2644 – 2654
- [4] Faouzi Nasri, Chaouki Ali and Habib Ben Bacha, A Review of Solar Thermal Electricity Production, International Journal of Research and Reviews in Applied Sciences, 8(3), September 2011, 349- 355.
- [5] Gerald Müller, Low Pressure Solar Thermal Converter, Renewable Energy, 35(1), 2010, 318–321.
- [6] Anyaka, Boniface Onyemachi, Nwokolo, Eric O, Solar Cells Technology: An Engine for National Development, IOSR Journal of Electrical and Electronics Engineering (IOSR-JEEE), 7(5), Sep. - Oct. 2013, 13-18.
- [7] Bettin Mironov, Application of Programmable Unijunction Transistor for Converting the Analog Signal of Semiconductor Sensor in a Frequency-Modulated Pulse Sequence, Proc. 8th International Conf. on Microelectronics and Computer Science, Chisinau, Republic of Moldova, October 22-25, 2014, 28-30.

- [8] G. G. Babichev, S. I. Kozlovskiy, V. A. Romanov, and N. N. Sharan, A Silicon Stress-Sensitive Unijunction Transistor, *Technical Physics*, 47(4), 2002, 436–441.
- [9] Satyasai Jagannath Nanda, Sasmita Kumari Behera and Ganapati Panda, Development of a Nonlinear Model of Unijunction Transistor Using Artificial Immune System, *Proc. IEEE Conf. World Congress on Nature & Biologically Inspired Computing*, Coimbatore, India, 9-11 Dec. 2009, 725-730.
- [10] James M. Conrad, Jonathan W. Mills, *STIQUITO: Advanced Experiments with a Simple and Inexpensive Robot*, 1st Edition, Ch. 16, Wiley-IEEE Computer Society Press, 1999.
- [11] Dewdney, A.K., Photovores: Intelligent Robots are Constructed From Castoffs, *Scientific American*, 267(3), Sept 1992, 42(1).
- [12] Aishwarya, R., et al., Solar Powered Stirling Engine for Self-Generating electricity, *IEEE International Conf. on Recent Advancements in Electrical, Electronics and Control Engineering*, Sivakasi, 15-17 Dec. 2011, 442 – 447.
- [13] P. Asgaonkar, Design of an Efficient Solar Engine Circuit for Autonomous Robotics, *International Journal of Computer Applications*, 7(7), October 2010, 1-4.
- [14] Kongtragool, and S. Wongwises, A Review of Solar - Powered Stirling Engines and Low Temperature Differential Stirling Engines, *Renewable and Sustainable Energy Reviews*, 7(2), 2003, 131-154.
- [15] M. A. Islam, S. Rahman and P. K. Halder, Design, Construction and Performance Test of a Ltd Stirling Engine, *Proc. of the Global Engineering, Science and Technology Conf.*, Dhaka, Bangladesh, 28-29 Dec. 2012, 1-10.
- [16] B. Chu, K. Jung, M.-Taeg Lim, and D. Hong, Robot-Based Construction Automation: An Application to Steel Beam Assembly (Part I), *Automation in Construction*, 32, July 2013, 46–61.
- [17] Siddarth Jain and Navneet Tiwar, BEAM Dragster Solar Robot with its Strategic Winning Design Analysis for the Nexus Photoroller Competition, *International Journal of Computer Applications*, 1(28), 2010, 75-80.
- [18] M. D. Singh, *Power Electronics*, 2nd Edition, Ch. 3, Tata McGraw-Hill Education, New Delhi, 2007.
- [19] L. Agrawal, D. P. Saha, R. Swami and R. P. Singh., Digital Magnetic Fluxmeter Using Unijunction Transistor Probe, *International Journal of Electronics*, 63(6), 1987, 905-910.
- [20] Dan steinhoff, John F. Burgess, *Small Business Management Fundamentals*, 2nd Edition, Tata Mc Graw-Hill Education, 2007, 87-97.
- [21] Green, M. A., Crystalline and Thin-Film Silicon Solar Cells: State of the Art and Future Potential, *Solar Energy*, 74(3), 2003, 181-192.
- [22] Shah, A. V., et al., Material and Solar Cells Research in Micro-Crystalline Silicon, *Solar Energy Materials and Solar Cells*, 78 (1-4), 2003, 469–491.
- [23] T. Saga, *Advances in Crystalline Si - Solar Cell Technology for Industrial Mass Production*, *NPG Asia Materials*, 2(3), 2010, 96–102.